Journal of Inflammation Research

Dovepress
open access to scientific and medical research

Open Access Full Text Article

ORIGINAL RESEARCH

HSP90-Dependent Upregulation of EZH2 Promotes Hypoxia/Reoxygenation-Induced Pyroptosis by Inhibiting miR-22 in Endothelial Cells

Paihe Deng, Huimin Hu

Clinical Laboratory Medicine Center, The Second Affiliated Hospital of Nanjing Medical University, Nanjing, Jiangsu, 210011, People's Republic of China

Correspondence: Huimin Hu, Clinical Laboratory Medicine Center, The Second Affiliated Hospital of Nanjing Medical University, 121 Jiangjiayuan Road, Nanjing, Jiangsu, 210011, People's Republic of China, Tel +86 1385 1616 797, Email hhm13851616797@163.com

Objective: Endothelial cell pyroptosis induced by hypoxia/reoxygenation (H/R) plays a key role in the pathogenesis of myocardial infarction (MI). However, the underlying mechanism is not clearly elucidated.

Methods: Human umbilical vein endothelial cells (HUVECs) exposed to H/R acted as in vitro model to investigate the mechanism of H/R-induced endothelial cell pyroptosis. CCK-8 assays were performed to investigate the viability of HUVECs. Calcein-AM/PI staining was carried out to quantify the death of HUVECs. The expression level of miR-22 was measured by RT-qPCR. The protein expression levels of zeste 2 polycomb repressive complex 2 subunit (EZH2), NLRP3, cleaved caspase-1 (c-caspase-1), GSDMD-N and heat shock protein 90 (HSP90) were measured by Western blot. Levels of IL-1β and IL-18 in culture medium were detected by ELISA. The intracellular localization of EZH2 was detected by immunofluorescence staining. Chromatin immunoprecipitation (ChIP) assay was used to detect the enrichment of EZH2 and H3K27me3 in the miR-22 promoter region. The binding between miR-22 and NLRP3 in HUVECs was confirmed by the dual luciferase assay. Reciprocal coimmunoprecipitation was conducted to detect the direct interaction between HSP90 and EZH2.

Results: H/R increased EZH2 expression, and the EZH2 siRNA could inhibit H/R-induced pyroptosis in HUVECs. H/R reduced miR-22 expression, which was reversed by EZH2 siRNA. Silencing of miR-22 by its inhibitor reversed EZH2 siRNA-induced pyroptosis inhibition in H/R-exposed HUVECs. Upregulation of miR-22 by its mimic suppressed EZH2 overexpression-enhanced pyroptosis in H/R-exposed HUVECs. ChIP assay confirmed that EZH2 bound to the miR-22 promoter region and repressed miR-22 expression through H3K27me3. Furthermore, luciferase reporter assay indicated that NLRP3 was a direct target of miR- 22 in HUVECs. Finally, HSP90 siRNA inhibited H/R-induced EZH2 expression, miR-22 downregulation, and pyroptosis in HUVECs.

Conclusion: H/R induces pyroptosis via the HSP90/EZH2/miR-22/NLRP3 signaling axis in endothelial cells.

Keywords: HSP90, EZH2, miR-22, pyroptosis, endothelial cells

Introduction

Increasing evidence indicates that cardiovascular disease is the leading global cause of death.[1] Myocardial infarction (MI) is the major cause of death in cardiovascular disease and has attracted widespread attention due to its increasing incidence, complications, poor outcomes and limited treatment.[2] Vascular endothelial cells play a key role in maintaining and supporting coronary microvessels and adjacent cardiomyocytes under normal conditions and angiogenesis under pathophysiological conditions.[3] Vascular endothelial cells have been shown to be sensitive to ischemic and reperfusion (I/R)-induced insult and I/R-induced vascular endothelial cell injury is a crucial and initial stage for the development of MI.[4–6] Therefore, exploring the molecular etiology of I/R-induced vascular endothelial cell injury of great significance to develop more effective treatment strategies for MI.

Pyroptosis, a form of proinflammatory cell death, is mediated by NOD-like receptor thermal protein domain associated protein 3 (NLRP3)-dependent inflammasome assembly, which is accompanied by gasdermin-D (GSDMD)

Received: 4 January 2023
Accepted: 15 June 2023
Published: 19 June 2023

cleavage and Interleukin-1β (IL-1β) and Interleukin-18 (IL-18) release.[7,8] Pyroptosis has been demonstrated to aggravate hypoxia/reoxygenation (H/R)-induced injury in various cells, including endothelial cells.[9,10] Recently, pyroptosis-associated endothelial cell death is significant in the development of MI.[11,12] Furthermore, by reducing vascular endothelial cell pyroptosis, chitosan hydrogel has been shown to increase the efficiency of bone marrow mesenchymal stem cells in the treatment of MI.[13] These findings indicated that the inhibition of I/R-induced endothelial cell pyroptosis could be a potential strategy for the treatment of MI. However, the molecular mechanisms underlying H/R-induced pyroptosis in vascular endothelial cells remain largely unknown.

MicroRNAs (miRNAs) are a highly conserved group of small endogenous non-coding RNA molecules composed of 21–23 nucleotides.[14,15] They act as post-transcriptional regulators of gene expression via binding to the partial sequence homology of the 3′-untranslated region of their target mRNAs.[14,15] miRNAs have been shown to be involved in the regulation of many biological processes, such as cancer, metabolism and inflammation.[14,15] Accumulating evidence has suggested that miRNAs are key regulators of pyroptosis.[16–18] Recently, miR-22 was reported to play a key role in the regulation of pyroptosis in different types of cells, including endothelial cells.[19–22] However, whether miR-22 mediates pyroptosis in H/R-induced pyroptosis in endothelial cells and the underlying mechanism are unclear.

Enhancer of zeste homolog 2 (EZH2), the enzymatic catalytic subunit of polycomb repressive complex 2 (PRC2), regulates gene expression epigenetically by catalyzing histone H3 lysine 27 (H3K27) trimethylation (H3K27me3).[23–25] An extensive number of studies have shown that EZH2 functions in various biological processes. For example, EZH2 was shown to inhibit cellular senescence and promote DNA damage repair.[26] EZH2 was also demonstrated to work as a master regulator of apoptosis, autophagy, and cell cycle progression.[25,27] In addition, EZH2 played a critical role in cell lineage determination and relative signaling pathways.[28] Recently, EZH2 was shown to promote oxidative stress-mediated renal pyroptosis.[29] However, the role of EZH2 in H/R-induced endothelial cell pyroptosis still remains unclear.

In this study, we used an in vitro model of H/R-exposed human umbilical vein endothelial cells (HUVECs) to simulate the in vivo vascular endothelial I/R and explore the role of EZH2 in H/R-induced vascular endothelial cell pyroptosis as well as its link with miR-22.

Materials and Methods

Cell Culture and Treatment

HUVECs (Cat. No. BNCC342247) were purchased from BeNa culture collection (Henan, China) and cultured in endothelial cell medium (ECM, Cat. No.1001, Sciencell, USA) containing 10% fetal bovine serum (FBS, Cat. No. 0025, Sciencell), 1% endothelial cell growth supplement (ECGS, Cat. No. 1052, Sciencell) and 1% penicillin/streptomycin (P/S, Cat. No. 0503, Sciencell) at 37°C, 5% CO_2. For H/R induction, HUVECs were cultured in glucose-free and serum-free medium and then transferred to the AnaeroPack^{TM} container (Mitsubishi Gas Chemical, Tokyo, Japan) containing a mixture of 1% O_2, 94% N_2 and 5% CO_2 at 37 °C for 12 h to establish hypoxia. Subsequently, the cells were cultured in normal DMEM with 10% FBS for 4 h to establish reoxygenation.

Cell Viability Assay

The viability of HUVECs was evaluated by using a CCK-8 assay kit (Cat. No. C0037, Beyotime, Shanghai, China) according to the manufacturer's instructions. HUVECs were treated as described in the text and then cultured into 96-well plates at a density of 5×10^3 cells/well. CCK-8 reagent (10 μL/well) was then added to the culture medium and continuously incubated for 2 h at 37 °C. The absorbance was determined at 450 nm using a microplate reader (ELx800, BioTek Instruments, Inc., Vermont, USA).

Calcein-AM/Propidium Iodide (PI) Staining

The treated HUVECs were analyzed with a Calcein-AM/PI cell viability/cytotoxicity assay kit (Cat. No. C2015M, Beyotime) according to the manufacturer's instructions. Briefly, after different stimulation, HUVECs were stained with Calcein-AM/PI at 37 °C for 30 min in the dark. Subsequently, the fluorescence images were acquired by using a fluorescence microscope (Leica DM2500). Image Pro advanced software was used to analyze the average fluorescence intensity.

ELISA Assay

After different stimulation, culture supernatants of HUVECs were collected and the concentrations of IL-1β and IL-18 in the supernatants were quantified by using commercial ELISA kits (IL-18, Cat. No. EMC011.96; IL-1β, Cat. No. EMC001b.96.2, NeoBioscience, Shenzhen, China) according to the manufacturer's instructions.

Western Blot

After different treatment, total protein was extracted from HUVECs using RIPA lysis buffer (Cat. No. P0013C, Beyotime). The protein concentrations were detected with an enhanced BCA protein assay kit (Cat. No. P0010, Beyotime). 30 μg of proteins was separated by SDS-PAGE, and subsequently transferred to polyvinylidene difluoride (PVDF) membranes. The membranes were blocked with 5% fat-free milk for 1 h at room temperature. The membranes were then incubated overnight at 4 °C with primary antibodies. The primary antibodies were purchased from Cell Signaling Technology (Danvers, MA, USA) and the dilution ratios of antibodies were as follows: NLRP3 (Cat. No. #15101, dilution 1/1000), cleaved caspase-1 (Cat. No. #4199, dilution 1/2000), GSDMD-N (Cat. No. #36425, dilution 1/2000), HSP90 (Cat. No. #4877, dilution 1/1000), EZH2 (Cat. No. #5246, dilution 1/1000), H3K27me3 (Cat. No. #9733, dilution 1/1000) and GAPDH (Cat. No. #5174, dilution 1/3000). After being washed three times with TBST, the membranes were incubated with secondary antibodies (Cat. No. sc-2004, Santa Cruz Technology, USA) for 1 h at room temperature. Protein bands were detected using enhanced chemiluminescence (ECL) reagent (Cat. No. 34577, Thermo Fisher Scientific, USA).

Immunofluorescence Staining

HUVECs were cultured under normal conditions or subjected to H/R exposure. After that cells were washed three times by PBS and then fixed with 4% paraformaldehyde for 30 min at room temperature. After being washed three times by PBS, the cells were treated with 0.2% Triton X-100 for 5 min at room temperature. The cells were washed three times by PBS followed by blocking in 1% BSA for 1 h at room temperature. Subsequently, the cells were incubated with antibody against EZH2 (Cat. No. #5246, dilution 1/200) or caspase-1 (Cat. No. #4199, dilution 1/200) overnight at 4° C. After that, the cells were incubated with the secondary antibodies Alex Fluor®488-labeled secondary antibody (green, A11008, 1:1000; Invitrogen, USA) at 37° C for 1 h. Finally, the cells were stained with DAPI blue (1:1000; cat. 0100–20, Southern Biotech, USA) for 5 min. Slides were observed by a fluorescent microscope (Leica DM2500).

RT-qPCR

Total RNA was extracted from HUVECs by using TRIzol (Invitrogen, USA) and was reverse-transcribed into cDNA using a reverse transcriptase kit (Cat. No. RR037A, TaKaRa, Tokyo, Japan) according to the manufacturer's instructions. Real-time qPCR was then carried out using SYBR premix Ex Taq II kit (Cat. No. RR390A, Tokyo, Japan) on an ABI 7300 Real-Time PCR system (Applied Biosystems, CA, USA). U6 was served as internal references and the relative expression level of miR-22 was calculated by $2^{-\Delta\Delta Ct}$ method. Primer sequences used were listed as follows: miR-22, forward: 5'-GGTTAAGCTGCCAGTTGAA-3' and reverse: 5'-CAGTGCGTGTCGTGGAGT-3'; U6 snRNA, forward: 5'- GCTTCGGCAGCACATATACTAAAAT-3' and reverse: 5'-CGCTTCACGAATTTGCGTGTCAT-3'.

siRNAs, Plasmid and Cell Transfection

Specific siRNAs for EZH2 and HSP90, miR-22 mimic, miR-22 inhibitor, control mimic, and control inhibitor were obtained from GenePharm (Shanghai, China). pcDNA3.1-HA plasmid with EZH2 overexpression (pcDNA3.1-HA-EZH2) was bought from Shanghai Genechem Co., Ltd. (Shanghai, China). Lipo6000™ (Cat. No. D2107, Beyotime) was used to transfect these oligonucleotides or plasmid into HUVECs following the protocol of the manufacturer. The corresponding sequences were as follows: siEZH2, 5′-CCAUGUUUACAACUAUCAA-3′; siHSP90-sense 5'-TCGTCAGAGCTGATGATGAAGT-3'; siNC, 5′-UUCUCCGAACGUGUCACGU-3'. The efficiency of transfection was validated by comparing the levels of EZH2 and HSP90 between transfected and controlled cells by Western blot.

Chromatin Immunoprecipitation (ChIP) Assay

ChIP assay was performed with ChIP assay kit (Cat. No. P2078, Beyotime, Shanghai, China) according to the manufacturer's instructions. Briefly, HUVECs were crosslinked with 1% formaldehyde for 10 minutes, and the reaction was quenched with glycine (0.125 mol/L) for 5 minutes. The cross-linked chromatin was then sonicated followed by immunoprecipitation with 10 mg of anti-EZH2 (Cat. No. #5246, CST), H3K27me3 (Cat. No. #9733, CST) or rabbit anti-IgG (Cat. No. A7016, Beyotime) overnight at 4 °C. After being purified, the enrichment of the miR-22 promoter was determined by qPCR. The corresponding primer sequences used were as follows: forward, 5'-ACTCTCGTTTGACGTAGCGCTT-3', and reverse, 5'-CGCCCTGGCTCTGATTGGCAAG-3'. The amount of immunoprecipitated DNA was calculated and then normalized to the amount of input DNA.

Dual Luciferase Assay

Double luciferase assay was used to detect the binding of miR-22 to NLRP3. The wild-type (WT) untranslated region or mutant (Mut) of NLRP3 was amplified and subcloned into a pGLuc-Dura-miR basic luciferase reporter vector (Cat. No. C0526, Beyotime). HUVECs were then cotransfected with the above two vectors and the miR-22 mimics or control mimic (mi-NC) using Lipo6000™ (Cat. No. D2107, Beyotime) according to the manufacturer's protocol. After 48 h, luciferase assays were performed using dual luciferase reporter gene assay kit (Cat. No. RG027, Beyotime). The luciferase activity was normalized to values of Renilla luciferase activity.

Co-Immunoprecipitation (Co-IP)

Co-IP was conducted by using immunoprecipitation kit (Cat. No. P2177S, Beyotime) according to the manufacturer's instructions. Briefly, after being treated as described in the text, 500 μg of total cellular proteins were extracted and used for immunoprecipitation by adding 1 μg of anti-HSP90 antibody (Cat. No. #4877, CST) and incubating at 4 °C for overnight. Immunoprecipitated proteins were analyzed by Western blot analysis with anti-EZH2 antibody (Cat. No. #5246, CST).

Statistical Analysis

All data are represented as the mean ± SD. Statistical analyses were carried out by using GraphPad Prism (version 9.0, USA). An unpaired Student's *t*-test was used to analyze the data between two groups. The differences among multiple groups were analyzed using one-way ANOVA followed by Tukey post hoc test. $P<0.05$ was considered to indicate a statistically significant difference.

Results

Hypoxia/Reoxygenation (H/R) Evokes Pyroptosis in HUVECs

To investigate the effect of H/R on the pyroptotic cell death of endothelial cells, HUVECs were subjected to hypoxia for 12 h and reoxygenation for 4 h. The results of the CCK-8 assay showed that H/R significantly reduced the viability of HUVECs (Figure 1A). Calcein-AM/PI staining showed that the percentage of PI positive cells was increased after H/R exposure (Figure 1B). Immunofluorescence showed that the core component caspase-1 was increased after H/R exposure (Figure 1C). H/R also increased the protein expression levels of pyroptosis-related proteins, including NLRP3, c-caspase-1, and GSDMD-N (Figure 1D). The results of ELISA assay showed that H/R increased IL-1β and IL-18 levels in the cell supernatants (Figure 1E). Collectively, these data suggest that H/R evokes pyroptosis in HUVECs.

Increased EZH2 Expression Promotes H/R-Induced Pyroptosis in HUVECs

To analyze the potential role of EZH2 in H/R-induced pyroptosis in HUVECs, the expression level of EZH2 in H/R-exposed HUVECs was firstly detected. As shown in Figure 2A, H/R significantly upregulated the expression level of EZH2 in HUVECs. The effect of EZH2 upregulation on H/R-induced pyroptosis was then investigated by transfecting HUVECs with EZH2 siRNA (siEZH2). As shown in Figure 2B, H/R-induced EZH2 upregulation was obviously inhibited by transfection with siEZH2. SiEZH2 also significantly reversed H/R-induced reduction in cell viability (Figure 2C) and increases in protein

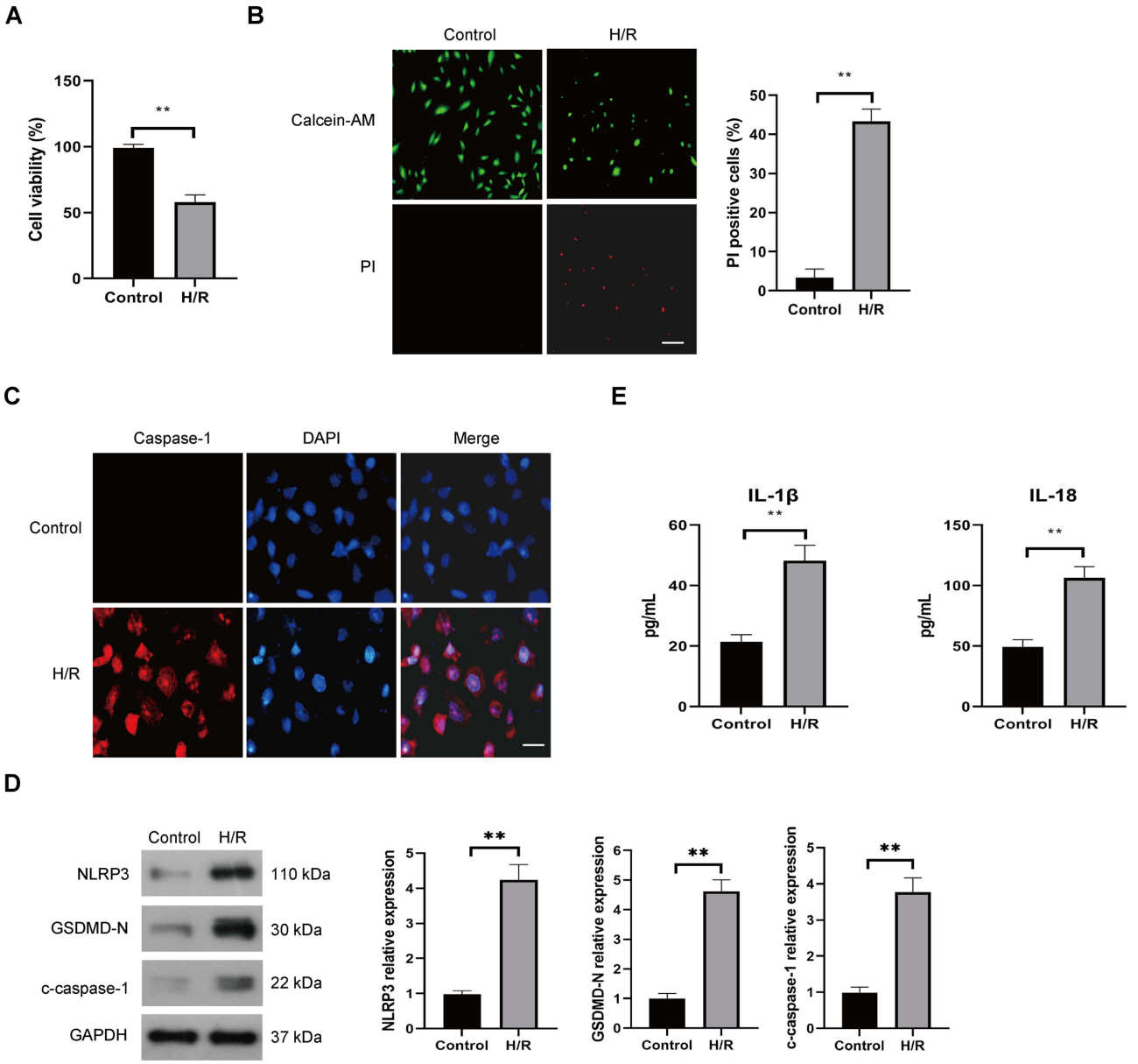

Figure 1 Effect of H/R on the pyroptotic cell death of endothelial cells. HUVECs were cultured under normal (control) conditions or subjected to hypoxia for 12 h and reoxygenation for 4 h (H/R). The viability of HUVECs was determined by the CCK-8 assay (**A**), the pyroptotic cell death was detected by calcein-AM/PI staining, the viable cells were stained with calcein-AM (green), whereas the dead cells were stained with PI (red), the dead cells (PI positive) were counted, Scale bar=100 μm (**B**), Immunofluorescence was used for detection of caspase-1, Scale bar=50 μm (**C**), the protein expression levels of, NLRP3, c-caspase-1, and GSDMD-N were examined by Western blot (**D**), the levels of secreted IL-1β and IL-18 were evaluated by ELISA (**E**). Data are presented as the means ± SD. **P<0.01, n=3.

expression levels of NLRP3, c-caspase-1, and GSDMD-N (Figure 2B). The secreted protein levels of IL-1β and IL-18 (Figure 2D) and PI-positive cells (Figure 2E) were significantly decreased by siEZH2 in H/R-exposed HUVECs. Taken together, these results indicate that H/R-induced EZH2 promotes pyroptosis in HUVECs.

EZH2 Promotes H/R-Induced Pyroptosis by Inhibiting miR-22 in HUVECs

The mechanism by which EZH2 promotes H/R-induced pyroptosis was then investigated. Recent studies revealed that EZH2 could regulate the expression level of miR-22,[30–32] which plays a key role in regulation of pyroptosis in various cells, including endothelial cells.[19,20,22] Thus, we investigated whether EZH2 promotes H/R-induced pyroptosis by modulating the expression level of miR-22. The results showed a significant decrease in miR-22 expression under H/R conditions (Figure 3A). EZH2 siRNA (siEZH2) significantly upregulated miR-22 expression in H/R-exposed HUVECs (Figure 3A).

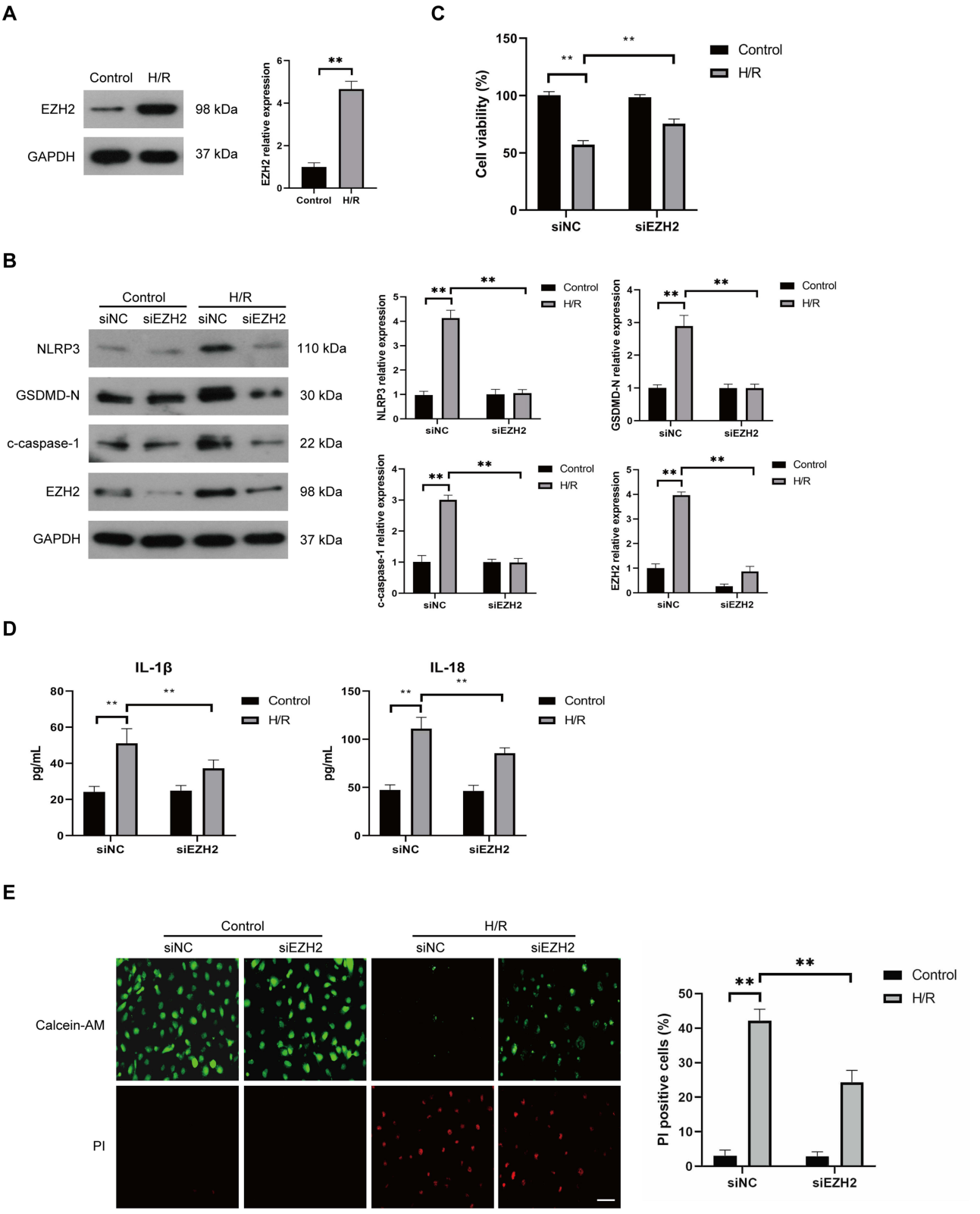

Figure 2 Knockdown of EZH2 represses H/R-induced pyroptosis in HUVECs. (**A**) The expression level of EZH2 in HUVECs was examined by Western blot under normal (control) and H/R conditions. (**B**–**E**) HUVECs were transfected with control siRNA (siNC) or EZH2 siRNA (siEZH2) and then cultured under normal (control) conditions or subjected to H/R exposure. The protein expression levels of EZH2, NLRP3, c-caspase-1, and GSDMD-N were examined by Western blot (**B**), the viability of HUVECs was determined by the CCK-8 assay (**C**), and the levels of secreted IL-1β and IL-18 were evaluated by ELISA (**D**), the pyroptotic cell death was detected by calcein-AM/PI staining, the viable cells were stained with calcein-AM (green), whereas the dead cells were stained with PI (red), the dead cells (PI positive) were counted, Scale bar=100 μm (**E**), Data are presented as the means ± SD.**P<0.01, n=3.

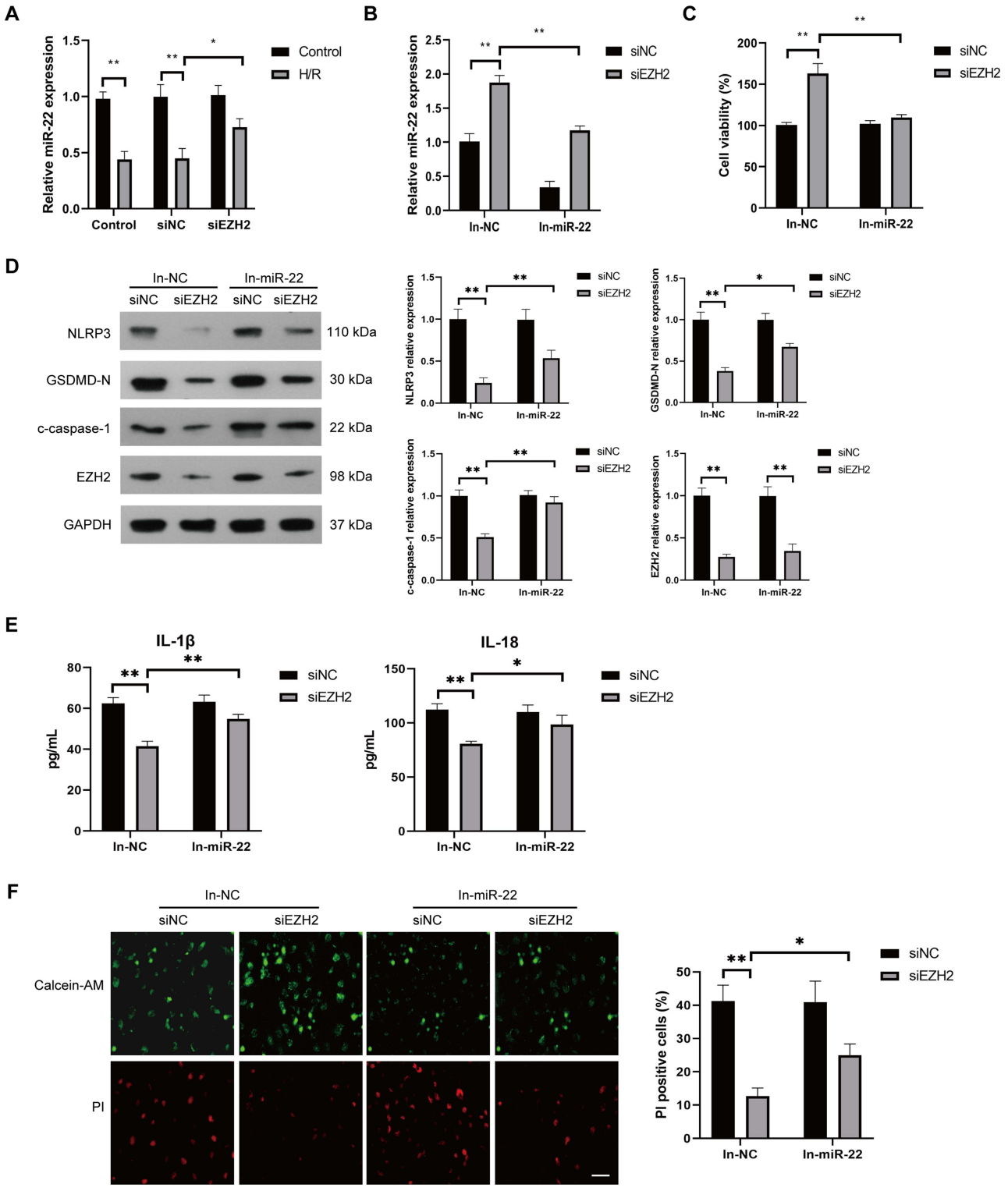

Figure 3 Inhibition of miR-22 suppresses EZH2 siRNA-induced pyroptosis inhibition in H/R-exposed HUVECs. (**A**) HUVECs were transfected with control siRNA (siNC) or EZH2 siRNA (siEZH2) and then cultured under normal (control) conditions or subjected to H/R exposure. The expression level of miR-22 in HUVECs was examined by RT-qPCR. (**B**–**F**) HUVECs were transfected with siNC or siEZH2 followed by treating with negative control inhibitor (In-NC) or miR-22 inhibitor (In-miR-22), and then subjected to H/R exposure. The expression level of miR-22 in HUVECs was examined by RT-qPCR (**B**), the viability of HUVECs was determined by the CCK-8 assay (**C**), the protein expression levels of EZH2, NLRP3, c-caspase-1, and GSDMD-N were examined by Western blot (**D**) and the levels of secreted IL-1β and IL-18 were evaluated by ELISA (**E**), the pyroptotic cell death was detected by calcein-AM/PI staining, the viable cells were stained with calcein-AM (green), whereas the dead cells were stained with PI (red), the dead cells (PI positive) were counted, Scale bar=100 μm (**F**), Data are presented as the means ± SD. *P<0.05, **P<0.01, n=3.

EZH2 knockdown cells that were treated with miR-22 inhibitor (In-miR-22) showed obvious decreases in miR-22 expression (Figure 3B) and viability of HUVECs under H/R conditions (Figure 3C). In-miR-22 also led to significant increases in expression levels of NLRP3, c-caspase-1 and GSDMD-N (Figure 3D), releases of IL-1β and IL-18 (Figure 3E), and PI-positive cells (Figure 3F) in siEZH2-transfected cells under H/R conditions.

The effect of miR-22 on EZH2-mediated pyroptosis were also investigated by treating EZH2- overexpressed HUVECs with miR-22 mimic (miR-22) under H/R conditions. As shown in Figure 4A, H/R exposure induced a significant decrease in miR-22 expression, which was further enhanced by EZH2 overexpression. miR-22 mimic (miR-22) remarkably increased the expression of miR-22 in EZH2-overexpressed HUVECs under H/R conditions (Figure 4B). miR-22 also reversed EZH2 overexpression-induced decrease in cell viability (Figure 4C) and increases in expression levels of NLRP3, c-caspase-1, GSDMD-N (Figure 4D), releases of IL-1β and IL-18 (Figure 4E) as well as PI-positive cells (Figure 4F) in H/R-exposed cells. Collectively, the above results indicate that EZH2 promotes H/R-induced pyroptosis by inhibiting miR-22 in HUVECs.

EZH2 Suppresses miR-22 Expression Through H3K27 Trimethylation in H/R-Exposed HUVECs

EZH2 was shown to inhibit many miRNAs expression through H3K27me3-mediated promoter histone methylation, including miR-22.[31–35] We then investigated whether EZH2 inhibits miR-22 expression through H3K27me3 in HUVECs. As shown in Figure 5A, H/R significantly increased the nuclear expression of EZH2. Chromatin immunoprecipitation (ChIP) assay showed that enrichment of EZH2 and H3K27me3 in the miR-22 promoter region was significantly increased after H/R exposure (Figure 5B). When the methyltransferase activity of EZH2 was silenced by its specific inhibitor, GSK126,[36,37] the expression level of H3K27me3 was obviously decreased, whereas the expression of EZH2 remained unchanged (Figure 5C). Notably, GSK126 treatment led to a significant increase in miR-22 expression in H/R-exposed HUVECs (Figure 5D). Furthermore, GSK126 treatment also significantly reduced the association of EZH2 with the promoter of miR-22 in H/R-exposed HUVECs (Figure 5E). Collectively, these results indicate that EZH2 suppresses miR-22 expression through H3K27me3 in H/R-exposed HUVECs.

miR-22 Directly Targets NLRP3 in HUVECs

It has been demonstrated that miR-22 suppressed NLRP3 expression through directly binding to the 3'-UTR of NLRP3 mRNA in various cells.[38,39] To confirm binding between miR-22 and NLRP3 in HUVECs, a dual luciferase assay was conducted. The results showed that miR-22 mimic (miR-22) significantly inhibited the luciferase activity of NLRP3 harboring wild type (WT) 3'UTR, but it had no effect on the luciferase activity of NLRP3 with mutant type (Mut) 3'UTR of NLRP3 (Figure 6A and B). Furthermore, the expression level of NLRP3 was obviously downregulated in H/R-exposed HUVECs after miR-22 mimic transfection (Figure 6C). In addition, miR-22 mimic obviously suppressed NLRP3 expression, whereas miR-22 inhibitor remarkably increased NLRP3 expression in HUVECs (Figure 6D). Collectively, these results demonstrate that miR-22 negatively regulates NLRP3 expression by directly targeting it in HUVECs.

HSP90 Contributes to H/R-Induced EZH2 Upregulation and Pyroptosis in HUVECs

Previous studies revealed that the protein stability and function of EZH2 were maintained by heat shock protein 90 (HSP90),[40,41] which also plays a critical role in the regulation of pyroptosis under different oxidative stress.[42,43] Thus, we investigated whether HSP90 contributes to H/R-induced EZH2 up-regulation and pyroptosis in endothelial cells. As shown in Figure 7A, H/R exposure significantly increased HSP90 expression in HUVECs. HSP90 siRNA (siHSP90) significantly reduced H/R-induced EZH2 upregulation in HUVECs (Figure 7A). Reciprocal coimmunoprecipitation revealed that HSP90 and EZH2 directly interacted with each other in H/R-exposed HUVECs (Figure 7B). Furthermore, siHSP90 significantly reversed H/R-induced downregulation of mi-22 (Figure 7C), decreased cell viability (Figure 7D), increased expression levels of NLRP3, c-caspase-1, GSDMD-N (Figure 7A), secreted protein levels of IL-

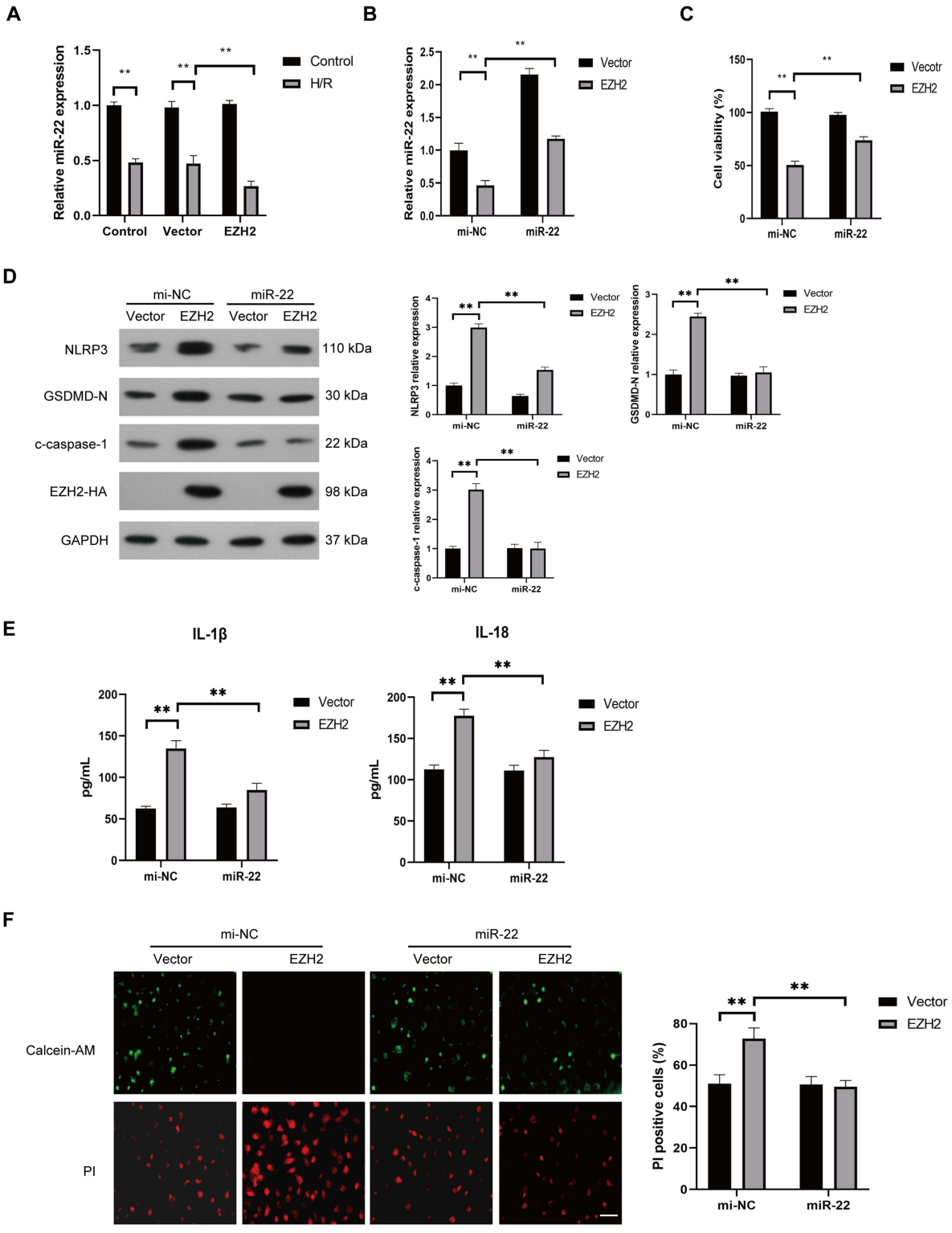

Figure 4 Upregulation of miR-22 suppresses EZH2 overexpression-enhanced pyroptosis in H/R-exposed HUVECs. (**A**) HUVECs were transfected with control plasmid (vector) or EZH2 overexpressed plasmid (EZH2) and then cultured under normal (control) conditions or subjected to H/R exposure. The expression level of miR-22 in HUVECs was examined by RT-qPCR. (**B**–**F**) HUVECs were transfected with vector or EZH2 followed by treating with control mimic (mi-NC) or miR-22 mimic (miR-22), and then subjected to H/R exposure. The expression level of miR-22 in HUVECs was examined by RT-qPCR (**B**), the viability of HUVECs was determined by the CCK-8 assay (**C**), the protein expression levels of EZH2, NLRP3, c-caspase-1, and GSDMD-N were examined by Western blot (**D**), the levels of secreted IL-1β and IL-18 were evaluated by ELISA (**E**), the pyroptotic cell death was detected by calcein-AM/PI staining, the viable cells were stained with calcein-AM (green), whereas the dead cells were stained with PI (red), the dead cells (PI positive) were counted, Scale bar=100 μm (**F**), Data are presented as the means ± SD. **P<0.01, n=3.

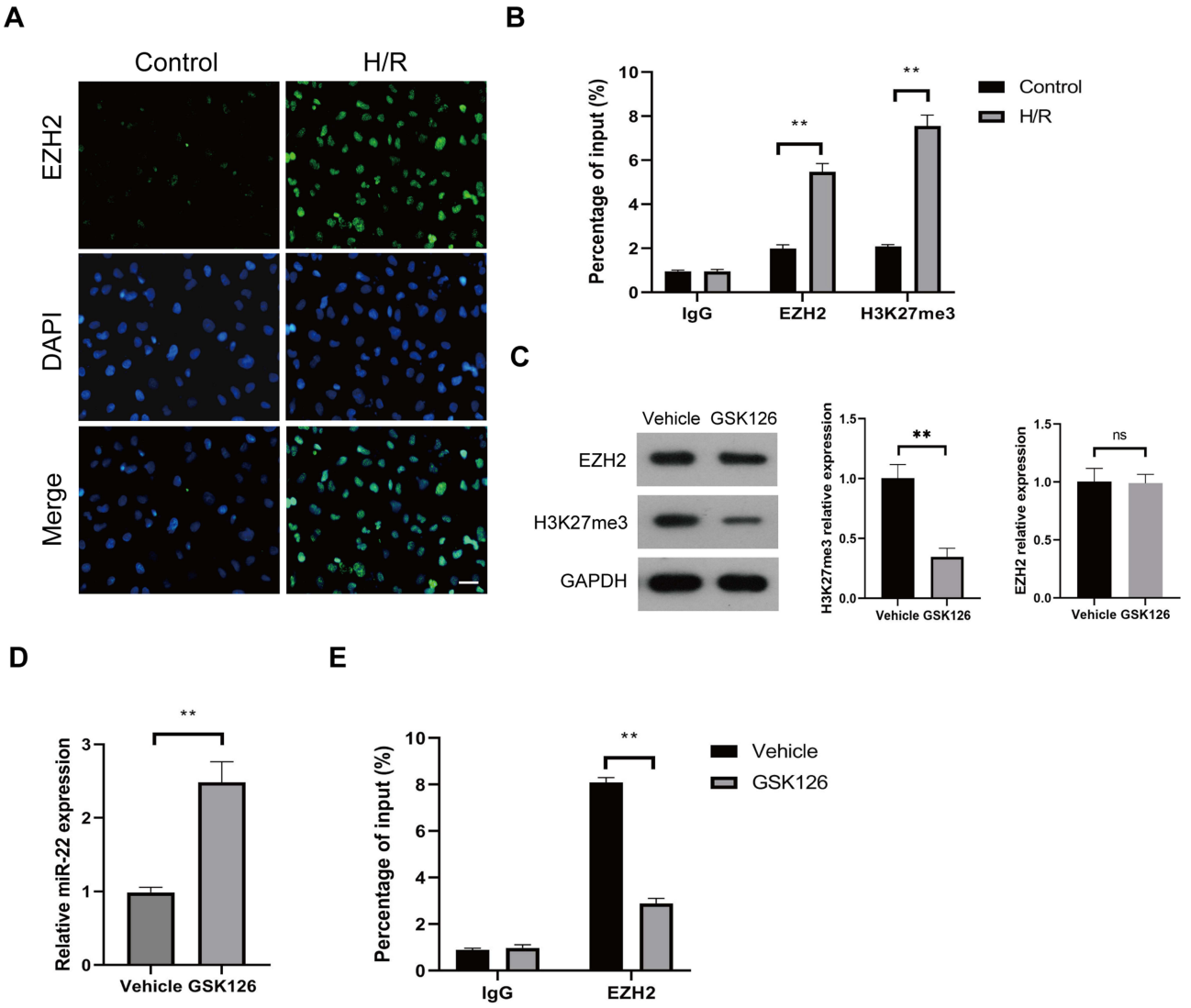

Figure 5 EZH2 represses miR-22 expression through H3K27me3 trimethylation in H/R-exposed HUVECs. (**A** and **B**) HUVECs were cultured under control or H/R conditions, and the intracellular localization of EZH2 was determined by IF (**A**), and the enrichments of EZH2 and H3K27me3 in miR-22 promoter were detected by chromatin immunoprecipitation (ChIP) assay (**B**). (**C**–**E**) HUVECs were treated with vehicle or GSK126 (5μM), and then cultured under H/R conditions. The expression levels of EZH2 and H3K27me3 were measured by Western blot (**C**), the expression level of miR-22 was determined by RT-qPCR (**D**), and the enrichment of EZH2 in miR-22 promoter was detected by ChIP assay (**E**). Scale bar: 100μm. Data are presented as the means ± SD. **P<0.01, ns, no significant, n=3.

1β and IL-18 (Figure 7E) as well as PI-positive cells (Figure 7F) in HUVECs. Collectively, these data indicate that HSP90 contributes to H/R-induced EZH2 upregulation and pyroptosis in HUVECs.

Discussion

Although EZH2 has been shown to play a crucial role in oxidative stress-mediated pyroptosis in human renal proximal tubular epithelial cells,[29] little is known about its role in H/R-induced endothelial cell pyroptosis. In the current study, we showed that H/R-induced EZH2 upregulation contributed to pyroptosis in endothelial cells. To our knowledge, the present study firstly reported the key role of EZH2 in endothelial cell pyroptosis under H/R conditions. Based on this, the mechanism by which EZH2 promotes H/R-induced pyroptosis was investigated.

It has been demonstrated that miRNAs act as key regulators of pyroptosis by modulating the expression levels of key genes in pyroptosis.[44–46] EZH2 was shown to suppress the expression of microRNAs under oxidative stress, such as miR-139,[47] miR-34a[35] and miR-451.[48] Recently, miR-22 was reported to promote endothelial cell pyroptosis.[19,20] Importantly, miR-22 was shown to be inhibited by EZH2 in various cells.[30–32] Consistent with these findings, we

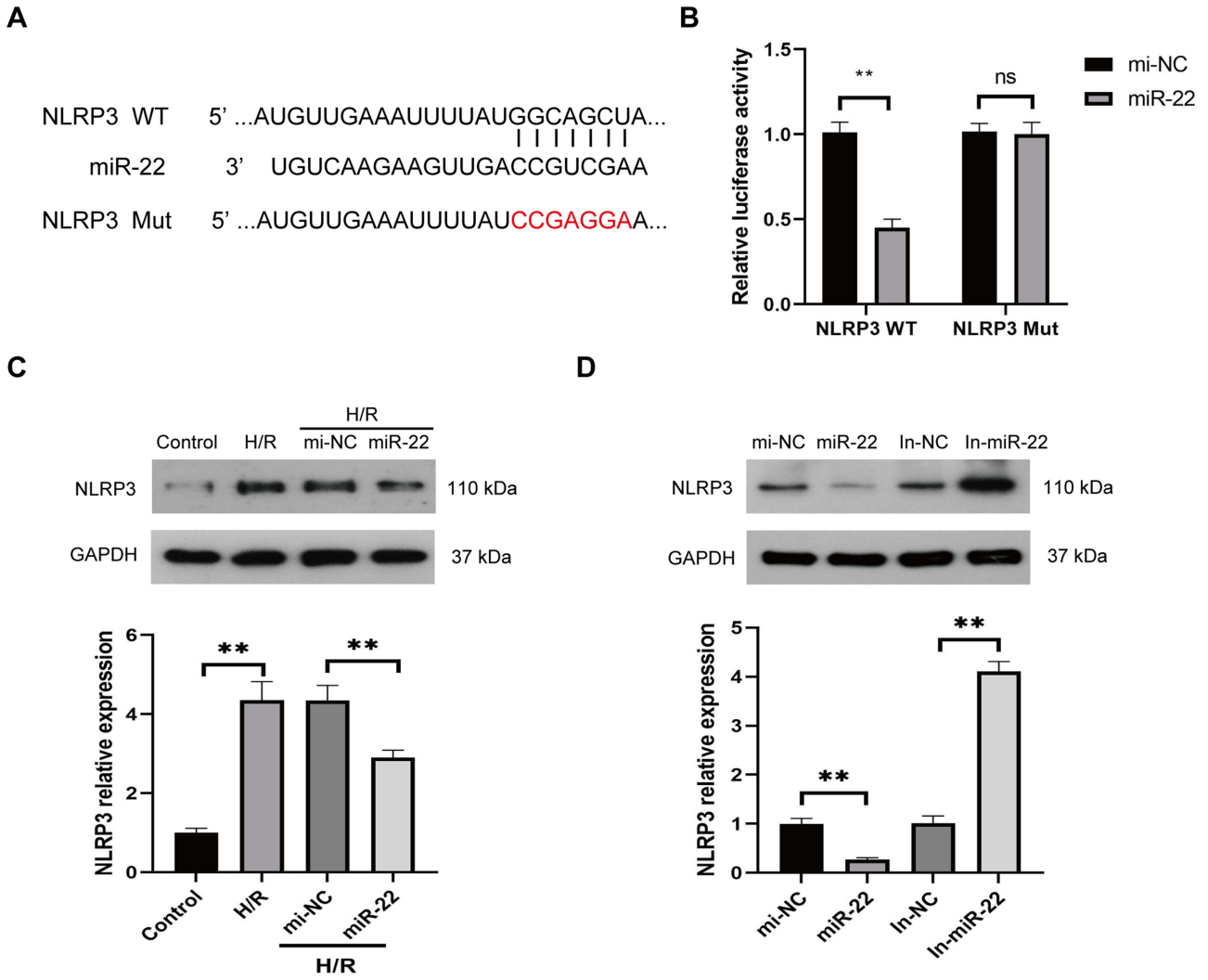

Figure 6 miR-22 directly targets NLRP3 in HUVECs. (**A**) Predicted binding sites between miR-22 and NLRP3. (**B**) Relative luciferase activity for NLRP3 WT and NLRP3 Mut. (**C**) Protein levels of NLRP3 in HUVECs transfected with miR-22 mimics (miR-22) or control mimics (mi-NC) under H/R conditions. (**D**) Protein levels of NLRP3 in HUVECs transfected with miR-22 mimics (miR-22), miR-22 inhibitor (In-miR-22), control mimics (mi-NC), or control inhibitor (In-NC). Data are presented as the means ± SD. **P<0.01, ns, no significant, n=3.

found that EZH2 promoted H/R-induced pyroptosis by inhibiting miR-22 in endothelial cells. However, it is undeniable that the pro-pyroptotic effects of EZH2 may be mediated by a variety of miRNAs in addition to miR-22 in H/R-exposed endothelial cells, and further investigation is required to uncover any other miRNAs involved.

Our results revealed that miR-22 mediates H/R-induced pyroptosis by directly targeting NLRP3 in HUVECs. This finding is consistent with previous studies that have shown NLRP3 is the direct target of miR-22 in other types of cells, such as neuronal cells, epithelial cells and cancer cells.[20,21,49] It is well known that miR-22 has many target genes, and the target gene that mediates the function of miR-22 depends on cell type and extracellular stress. To date, there is no other molecules are reported to be the targets of miR-22 and regulate pyroptosis in endothelial cells, except to NLRP3. Phosphatase and tensin homolog (PTEN), a tumor suppressor gene, has demonstrated to be the target gene of miR-22 in different types of cells.[50–52] Moreover, PTEN also plays a key role in pyroptosis in different types of cells, including endothelial cells.[53–55] Therefore, whether PTEN acts as the target of miR-22 during H/R-induced pyroptosis is another point for us to investigate in the near future.

H3K27me3 is an important epigenetic event associated with transcriptional silencing.[56,57] As a methyltransferase component of PRC2, EZH2 was reported to mediate epigenetic gene silencing through H3K27me3.[56,57] Emerging evidences suggested that EZH2 epigenetically silences miRNAs expression by trimethylating H3K27.[33–35] GSK126 is

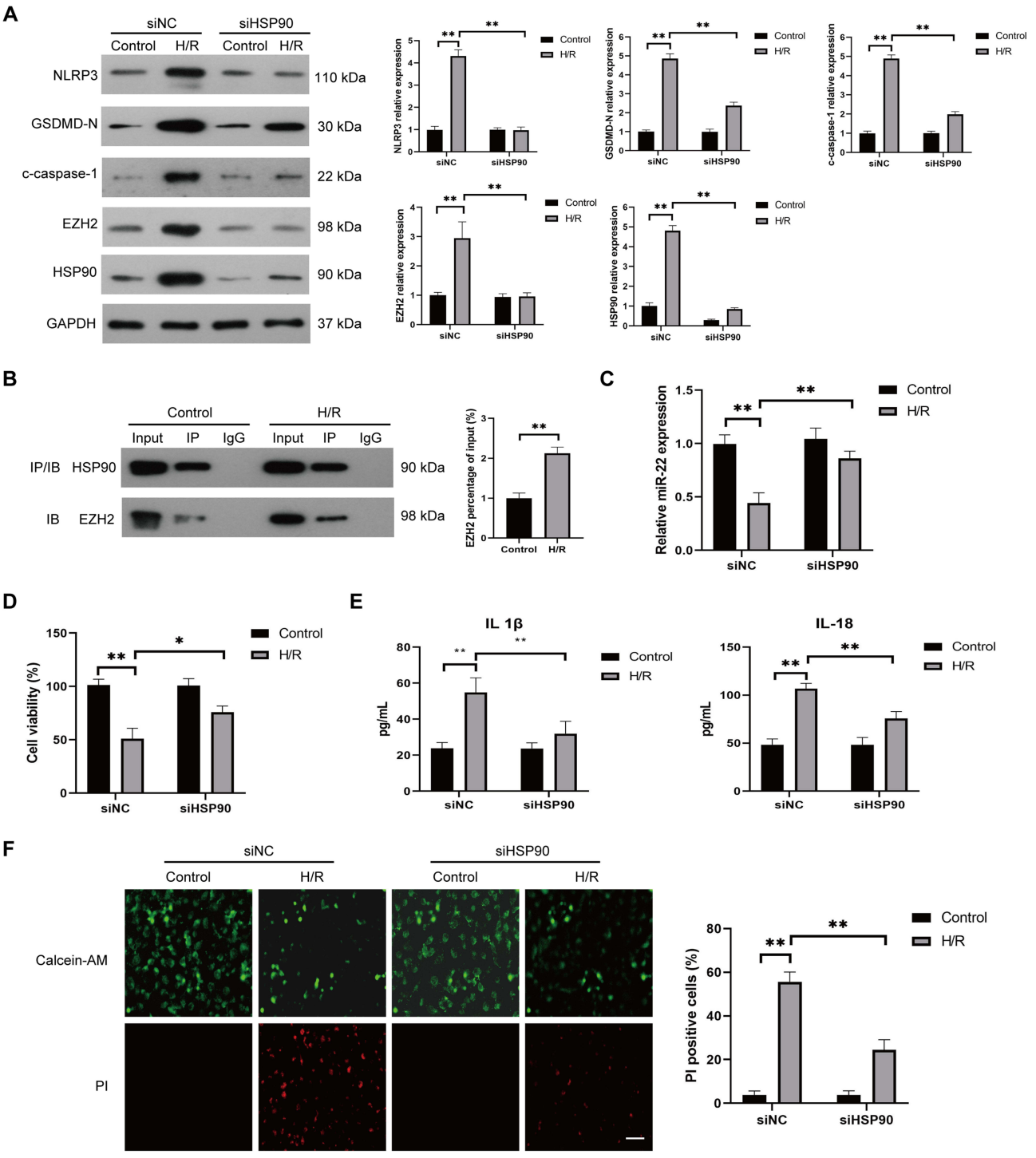

Figure 7 HSP90 is required for H/R-induced EZH2 upregulation and pyroptosis in HUVECs. (**A**) HUVECs were transfected with control siRNA (siNC) or HSP90 siRNA (siHSP90) and then cultured under control conditions or subjected to H/R exposure. The expression levels of HSP90, EZH2, NLRP3, c-caspase-1, and GSDMD-N were measured by Western blot. (**B**) The direct interaction between EZH2 and HSP90 in HUVECs after H/R exposure was determined by immunoprecipitation with anti-HSP90 antibody and analyzed by Western blot with anti-EZH2 antibody or anti-HSP90 antibody. (**C**–**F**) HUVECs were transfected with control siNC or siHSP90 and then cultured under control conditions or subjected to H/R exposure, the expression level of miR-22 was determined by RT-qPCR (**C**), the viability of HUVECs was determined by the CCK-8 assay (**D**), the levels of secreted IL-1β and IL-18 were evaluated by ELISA (**E**), the pyroptotic cell death was detected by calcein-AM/PI staining, the viable cells were stained with calcein-AM (green), whereas the dead cells were stained with PI (red), the dead cells (PI positive) were counted, Scale bar=100 μm (**F**), Data are presented as the means ± SD. *P<0.05, **P<0.01, n=3.

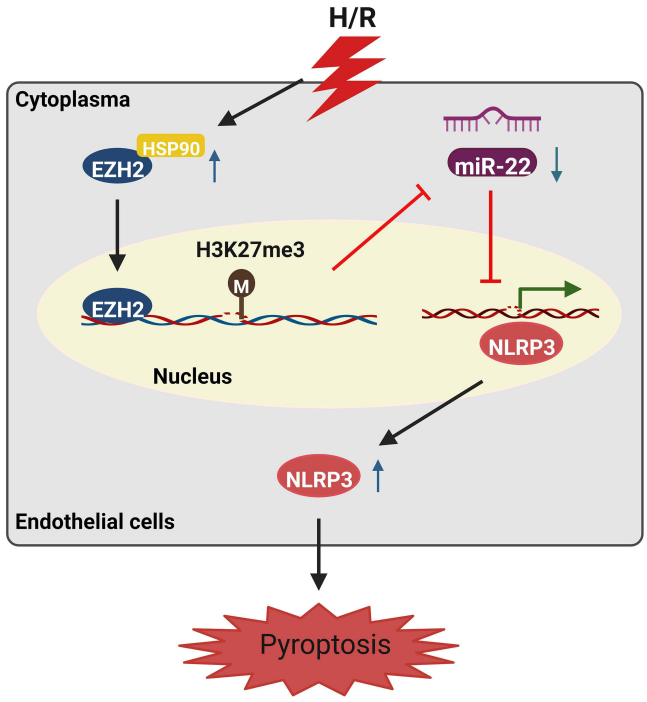

Figure 8 Schematic illustration of H/R-induced endothelial cell pyroptosis via the HSP90/EZH2/miR-22/NLRP3 signaling pathway.

a highly selective inhibitor of EZH2 methyltransferase activity that influences H3K27me3 chromatin content and transcriptional control.[36,37] Our experimental data showed that GSK126 not only reversed H/R-induced miR-22 downregulation, but also inhibited the binding of EZH2 to the promoter of miR-22, indicating that EZH2 inhibits miR-22 through H3K27me3 in H/R-exposed endothelial cells. MiR-22 expression has been reported to be inactivated by aberrant DNA methylation.[58] Furthermore, H3K27me3 and DNA methylation have been linked to establish and maintain gene silencing.[59] Thus, it will be interesting to investigate whether there is an epigenetic cross-talk between DNA methylation and H3K27me3 in silencing of miR-22 expression in H/R-exposed endothelial cells.

HSP90 is a molecular chaperone that facilitates the correct folding and functionality of its client protein through the binding of ATP molecule.[60] Previous reports revealed that HSP90 plays a crucial role in various diseases, such as cancer, lung injury and cardiovascular diseases.[60] HSP90 has been shown to stabilize EZH2 protein expression through the direct interaction with EZH2.[40,41] In agreement with these previous studies, our experimental results showed that HSP90 and EZH2 directly interacted with each other in H/R-exposed HUVECs. Recently, inhibition of HSP90 was reported to suppress pyroptosis in THP-1 cells.[42] Consistently, we found that HSP90 suppression increased miR-22 expression and inhibited pyroptosis in H/R-exposed HUVECs. These findings suggest that HSP90 facilitates H/R-induced pyroptosis in endothelial cells through EZH2-mediated miR-22 downregulation.

Conclusion

In conclusion, the current study demonstrated that EZH2, which is upregulated in H/R-exposed HUVECs in a HSP90-dependent manner, represses miR-22 through H3K27me3, thereby elevating NLRP3 to facilitate pyroptosis (Figure 8). These findings shed light on the molecular mechanisms of H/R-evoked pyroptosis of endothelial cells. However, an in vivo study is still needed to confirm our findings.

Abbreviations

H/R, hypoxia/reoxygenation; EZH2, enhancer of zeste 2 polycomb repressive complex 2 subunit; HUVECs, human umbilical vein endothelial cells; ChIP, Chromatin immunoprecipitation; HSP90, heat shock protein 90; GSDMD, gasderminD; PRC2, polycomb repressive complex 2; H3K27, histone H3 lysine 27; MicroRNAs, miRNAs.

Data Sharing Statement

Data will be made available on request.

Author Contributions

All authors made a significant contribution to the work reported, whether that is in the conception, study design, execution, acquisition of data, analysis, and interpretation, or in all these areas; took part in drafting, revising, or critically reviewing the article; gave final approval of the version to be published; have agreed on the journal to which the article has been submitted; and agree to be accountable for all aspects of the work.

Disclosure

The authors report no conflicts of interest in this work.

References

1. Akhmerov A, Parimon T. Extracellular vesicles, inflammation, and cardiovascular disease. *Cells*. 2022;11(14):2229. doi:10.3390/cells11142229
2. Lu Y, Luo Y, Zhu R, Huang X, Bai S. Advanced bioactive hydrogels for the treatment of myocardial infarction. *J Mater Chem B*. 2022;10(41):8375–8385. doi:10.1039/d2tb01591a
3. Liao Z, Chen Y, Duan C, et al. Cardiac telocytes inhibit cardiac microvascular endothelial cell apoptosis through exosomal miRNA-21-5p-targeted cdip1 silencing to improve angiogenesis following myocardial infarction. *Theranostics*. 2021;11(1):268–291. doi:10.7150/thno.47021
4. Wu X, Zhang H, Qi W, et al. Nicotine promotes atherosclerosis via ROS-NLRP3-mediated endothelial cell pyroptosis. *Cell Death Dis*. 2018;9(2):171. doi:10.1038/s41419-017-0257-3
5. Penna C, Femmino S, Caldera F, et al. Cyclic nigerosyl-nigerose as oxygen nanocarrier to protect cellular models from hypoxia/reoxygenation injury: implications from an in vitro model. *Int J Mol Sci*. 2021;22(8):4208. doi:10.3390/ijms22084208
6. Zhou R, Huang W, Fan X, et al. miR-499 released during myocardial infarction causes endothelial injury by targeting alpha7-nAchR. *J Cell Mol Med*. 2019;23(9):6085–6097. doi:10.1111/jcmm.14474
7. Zheng Z, Li G. Mechanisms and therapeutic regulation of pyroptosis in inflammatory diseases and cancer. *Int J Mol Sci*. 2020;21(4):1456. doi:10.3390/ijms21041456
8. Yu P, Zhang X, Liu N, Tang L, Peng C, Chen X. Pyroptosis: mechanisms and diseases. *Signal Transduct Target Ther*. 2021;6(1):128. doi:10.1038/s41392-021-00507-5
9. Qiu Z, He Y, Ming H, Lei S, Leng Y, Xia ZY. Lipopolysaccharide (LPS) aggravates high glucose- and hypoxia/reoxygenation-induced injury through activating ROS-dependent NLRP3 inflammasome-mediated pyroptosis in H9C2 cardiomyocytes. *J Diabetes Res*. 2019;2019:8151836. doi:10.1155/2019/8151836
10. Yao T, Song Y, Li S, Gu J, Yan X. Inhibition of lncRNA NEAT1 protects endothelial cells against hypoxia/reoxygenation induced NLRP3 inflammasome activation by targeting the miR204/BRCC3 axis. *Mol Med Rep*. 2022;25(1). doi:10.3892/mmr.2021.12548
11. Sun W, Lu H, Dong S, et al. Beclin1 controls caspase-4 inflammsome activation and pyroptosis in mouse myocardial reperfusion-induced microvascular injury. *Cell Commun Signal*. 2021;19(1):107. doi:10.1186/s12964-021-00786-z
12. Zhang B, Liu G, Huang B, et al. KDM3A attenuates myocardial ischemic and reperfusion injury by ameliorating cardiac microvascular endothelial cell pyroptosis. *Oxid Med Cell Longev*. 2022;2022:4622520. doi:10.1155/2022/4622520
13. Liu Y, Li P, Qiao C, et al. Chitosan hydrogel enhances the therapeutic efficacy of bone marrow-derived mesenchymal stem cells for myocardial infarction by alleviating vascular endothelial cell pyroptosis. *J Cardiovasc Pharmacol*. 2020;75(1):75–83. doi:10.1097/FJC.0000000000000760
14. Pelletier D, Rivera B, Fabian MR, Foulkes WD. miRNA biogenesis and inherited disorders: clinico-molecular insights. *Trends Genet*. 2023;39(5):401–414. doi:10.1016/j.tig.2023.01.009
15. Diener C, Keller A, Meese E. Emerging concepts of miRNA therapeutics: from cells to clinic. *Trends Genet*. 2022;38(6):613–626. doi:10.1016/j.tig.2022.02.006
16. Wang F, Gu L, Wang Y, et al. MicroRNA-122a aggravates intestinal ischemia/reperfusion injury by promoting pyroptosis via targeting EGFR-NLRP3 signaling pathway. *Life Sci*. 2022;307:120863. doi:10.1016/j.lfs.2022.120863
17. Miao Z, Miao Z, Teng X, Xu S. Chlorpyrifos triggers epithelioma papulosum cyprini cell pyroptosis via miR-124-3p/CAPN1 axis. *J Hazard Mater*. 2022;424(Pt A):127318. doi:10.1016/j.jhazmat.2021.127318
18. Heo MJ, Kim TH, You JS, Blaya D, Sancho-Bru P, Kim SG. Alcohol dysregulates miR-148a in hepatocytes through FoxO1, facilitating pyroptosis via TXNIP overexpression. *Gut*. 2019;68(4):708–720. doi:10.1136/gutjnl-2017-315123
19. Chi K, Geng X, Liu C, et al. LncRNA-HOTAIR promotes endothelial cell pyroptosis by regulating the miR-22/NLRP3 axis in hyperuricaemia. *J Cell Mol Med*. 2021;25(17):8504–8521. doi:10.1111/jcmm.16812
20. Zhang HS, Ouyang B, Ji XY, Liu MF. Gastrodin alleviates cerebral ischaemia/reperfusion injury by inhibiting pyroptosis by regulating the lncRNA NEAT1/miR-22-3p axis. *Neurochem Res*. 2021;46(7):1747–1758. doi:10.1007/s11064-021-03285-2
21. Song Z, Zhang Y, Gong B, Xu H, Hao Z, Liang C. Long noncoding RNA LINC00339 promotes renal tubular epithelial pyroptosis by regulating the miR-22-3p/NLRP3 axis in calcium oxalate-induced kidney stone. *J Cell Biochem*. 2019;120(6):10452–10462. doi:10.1002/jcb.28330
22. Song Y, Yang L, Guo R, Lu N, Shi Y, Wang X. Long noncoding RNA MALAT1 promotes high glucose-induced human endothelial cells pyroptosis by affecting NLRP3 expression through competitively binding miR-22. *Biochem Biophys Res Commun*. 2019;509(2):359–366. doi:10.1016/j.bbrc.2018.12.139
23. Wang J, Wang GG. No easy way out for EZH2: its pleiotropic, noncanonical effects on gene regulation and cellular function. *Int J Mol Sci*. 2020;21(24):9501. doi:10.3390/ijms21249501
24. Duan R, Du W, Guo W. EZH2: a novel target for cancer treatment. *J Hematol Oncol*. 2020;13(1):104. doi:10.1186/s13045-020-00937-8

25. Nutt SL, Keenan C, Chopin M, Allan RS. EZH2 function in immune cell development. *Biol Chem*. 2020;401(8):933–943. doi:10.1515/hsz-2019-0436
26. Ito T, Teo YV, Evans SA, Neretti N, Sedivy JM. Regulation of cellular senescence by polycomb chromatin modifiers through distinct DNA damage- and histone methylation-dependent pathways. *Cell Rep*. 2018;22(13):3480–3492. doi:10.1016/j.celrep.2018.03.002
27. Yao Y, Hu H, Yang Y, et al. Downregulation of Enhancer of Zeste Homolog 2 (EZH2) is essential for the induction of autophagy and apoptosis in colorectal cancer cells. *Genes*. 2016;7(10):83. doi:10.3390/genes7100083
28. Batool A, Jin C, Liu YX. Role of EZH2 in cell lineage determination and relative signaling pathways. *Front Biosci*. 2019;24(5):947–960. doi:10.2741/4760
29. Liu H, Chen Z, Weng X, et al. Enhancer of zeste homolog 2 modulates oxidative stress-mediated pyroptosis in vitro and in a mouse kidney ischemia-reperfusion injury model. *FASEB J*. 2020;34(1):835–852. doi:10.1096/fj.201901816R
30. Cai B, Li M, Zheng Y, et al. EZH2-mediated inhibition of microRNA-22 promotes differentiation of hair follicle stem cells by elevating STK40 expression. *Aging*. 2020;12(13):12726–12739. doi:10.18632/aging.103165
31. Chen S, Wang G, Tao K, et al. Long noncoding RNA metastasis-associated lung adenocarcinoma transcript 1 cooperates with enhancer of zeste homolog 2 to promote hepatocellular carcinoma development by modulating the microRNA-22/Snail family transcriptional repressor 1 axis. *Cancer Sci*. 2020;111(5):1582–1595. doi:10.1111/cas.14372
32. Wang C, Liu G, Yang H, et al. MALAT1-mediated recruitment of the histone methyltransferase EZH2 to the microRNA-22 promoter leads to cardiomyocyte apoptosis in diabetic cardiomyopathy. *Sci Total Environ*. 2021;766:142191. doi:10.1016/j.scitotenv.2020.142191
33. Gu X, Xu Y, Xue WZ, et al. Interplay of miR-137 and EZH2 contributes to the genome-wide redistribution of H3K27me3 underlying the Pb-induced memory impairment. *Cell Death Dis*. 2019;10(9):671. doi:10.1038/s41419-019-1912-7
34. Kwon H, Song K, Han C, et al. Epigenetic silencing of miRNA-34a in human cholangiocarcinoma via EZH2 and DNA methylation: impact on regulation of notch pathway. *Am J Pathol*. 2017;187(10):2288–2299. doi:10.1016/j.ajpath.2017.06.014
35. Lin JM, Hsu CH, Chen JC, Kao SH, Lin YC. BCL-6 promotes the methylation of miR-34a by recruiting EZH2 and upregulating CTRP9 to protect ischemic myocardial injury. *Biofactors*. 2021;47(3):386–402. doi:10.1002/biof.1704
36. Li Y, Gan Y, Liu J, et al. Downregulation of MEIS1 mediated by ELFN1-AS1/EZH2/DNMT3a axis promotes tumorigenesis and oxaliplatin resistance in colorectal cancer. *Signal Transduct Target Ther*. 2022;7(1):87. doi:10.1038/s41392-022-00902-6
37. Huang S, Wang Z, Zhou J, et al. EZH2 inhibitor GSK126 suppresses antitumor immunity by driving production of myeloid-derived suppressor cells. *Cancer Res*. 2019;79(8):2009–2020. doi:10.1158/0008-5472.CAN-18-2395
38. Hu Z, Lv X, Chen L, et al. Protective effects of microRNA-22-3p against retinal pigment epithelial inflammatory damage by targeting NLRP3 inflammasome. *J Cell Physiol*. 2019;234(10):18849–18857. doi:10.1002/jcp.28523
39. Yang K, Li W, Duan W, et al. Resveratrol attenuates pulmonary embolism associated cardiac injury by suppressing activation of the inflammasome via the MALAT1miR223p signaling pathway. *Int J Mol Med*. 2019;44(6):2311–2320. doi:10.3892/ijmm.2019.4358
40. Lee YC, Chang WW, Chen YY, et al. Hsp90alpha mediates BMI1 expression in breast cancer stem/progenitor cells through facilitating nuclear translocation of c-Myc and EZH2. *Int J Mol Sci*. 2017;18(9):1986. doi:10.3390/ijms18091986
41. Huang Q, He S, Tian Y, et al. Hsp90 inhibition destabilizes Ezh2 protein in alloreactive T cells and reduces graft-versus-host disease in mice. *Blood*. 2017;129(20):2737–2748. doi:10.1182/blood-2016-08-735886
42. Zhou Z, Li X, Qian Y, Liu C, Huang X, Fu M. Heat shock protein 90 inhibitors suppress pyroptosis in THP-1 cells. *Biochem J*. 2020;477(20):3923–3934. doi:10.1042/BCJ20200351
43. Bulek K, Zhao J, Liao Y, et al. Epithelial-derived gasdermin D mediates nonlytic IL-1beta release during experimental colitis. *J Clin Invest*. 2020;130(8):4218–4234. doi:10.1172/JCI138103
44. Zhang T, Wu DM, Luo PW, et al. CircNEIL3 mediates pyroptosis to influence lung adenocarcinoma radiotherapy by upregulating PIF1 through miR-1184 inhibition. *Cell Death Dis*. 2022;13(2):167. doi:10.1038/s41419-022-04561-x
45. Ye Y, Feng Z, Tian S, et al. HBO alleviates neural stem cell pyroptosis via lncRNA-H19/miR-423-5p/NLRP3 axis and improves neurogenesis after oxygen glucose deprivation. *Oxid Med Cell Longev*. 2022;2022:9030771. doi:10.1155/2022/9030771
46. Chu C, Wang B, Zhang Z, et al. miR-513c-5p suppression aggravates pyroptosis of endothelial cell in deep venous thrombosis by promoting caspase-1. *Front Cell Dev Biol*. 2022;10:838785. doi:10.3389/fcell.2022.838785
47. Zheng X, Zhao X, Han Z, Chen K. Enhancer of zeste homolog 2 participates in the process of atherosclerosis by modulating microRNA-139-5p methylation and signal transducer and activator of transcription 1 expression. *IUBMB Life*. 2021;73(1):238–251. doi:10.1002/iub.2423
48. Meng K, Jiao J, Zhu RR, et al. The long noncoding RNA hotair regulates oxidative stress and cardiac myocyte apoptosis during ischemia-reperfusion injury. *Oxid Med Cell Longev*. 2020;2020:1645249. doi:10.1155/2020/1645249
49. Xu Z, Xi K. LncRNA RGMB-AS1 promotes laryngeal squamous cell carcinoma cells progression via sponging miR-22/NLRP3 axis. *Biomed Pharmacother*. 2019;118:109222. doi:10.1016/j.biopha.2019.109222
50. Gao Y, Li X, Zeng C, et al. CD63(+) cancer-associated fibroblasts confer tamoxifen resistance to breast cancer cells through exosomal miR-22. *Adv Sci*. 2020;7(21):2002518. doi:10.1002/advs.202002518
51. Wang X, Wang Y, Kong M, Yang J. MiR-22-3p suppresses sepsis-induced acute kidney injury by targeting PTEN. *Biosci Rep*. 2020;40(6). doi:10.1042/BSR20200527
52. Li C, Zhang L, Bu X, Chu G, Zhao X, Liu Y. LncRNA NORAD promotes the progression of myocardial infarction by targeting the miR-22-3p/PTEN axis. *Acta Biochim Biophys Sin*. 2022;54(4):463–473. doi:10.3724/abbs.2022037
53. Zha X, Xi X, Fan X, Ma M, Zhang Y, Yang Y. Overexpression of METTL3 attenuates high-glucose induced RPE cell pyroptosis by regulating miR-25-3p/PTEN/Akt signaling cascade through DGCR8. *Aging*. 2020;12(9):8137–8150. doi:10.18632/aging.103130
54. Ning JZ, He KX, Cheng F, et al. Long non-coding RNA MEG3 promotes pyroptosis in testicular ischemia-reperfusion injury by targeting MiR-29a to modulate PTEN expression. *Front Cell Dev Biol*. 2021;9:671613. doi:10.3389/fcell.2021.671613
55. Wang JJ, Chen ZL, Wang DD, Wu KF, Huang WB, Zhang LQ. linc00174 deteriorates the pathogenesis of diabetic retinopathy via miR-26a-5p/PTEN/Akt signalling cascade-mediated pyroptosis. *Biochem Biophys Res Commun*. 2022;630:92–100. doi:10.1016/j.bbrc.2022.09.016
56. Li Y, Li H, Zhou L. EZH2-mediated H3K27me3 inhibits ACE2 expression. *Biochem Biophys Res Commun*. 2020;526(4):947–952. doi:10.1016/j.bbrc.2020.04.010

57. Liu X, Li C, Zhang R, et al. The EZH2- H3K27me3-DNMT1 complex orchestrates epigenetic silencing of the wwc1 gene, a Hippo/YAP pathway upstream effector, in breast cancer epithelial cells. *Cell Signal*. 2018;51:243–256. doi:10.1016/j.cellsig.2018.08.011
58. Yun J, Ji YS, Jang GH, et al. TET2 mutation and high miR-22 expression as biomarkers to predict clinical outcome in myelodysplastic syndrome patients treated with hypomethylating therapy. *Curr Issues Mol Biol*. 2021;43(2):917–931. doi:10.3390/cimb43020065
59. Vire E, Brenner C, Deplus R, et al. The polycomb group protein EZH2 directly controls DNA methylation. *Nature*. 2006;439(7078):871–874. doi:10.1038/nature04431
60. Sima S, Richter K. Regulation of the Hsp90 system. *Biochim Biophys Acta Mol Cell Res*. 2018;1865(6):889–897. doi:10.1016/j.bbamcr.2018.03.008